

## Estimating gas emissions from a farm with an inverse-dispersion technique

Thomas K. Flesch<sup>a,\*</sup>, John D. Wilson<sup>a</sup>, Lowry A. Harper<sup>b</sup>, Brian P. Crenna<sup>a</sup>

<sup>a</sup>Department of Earth and Atmospheric Sciences, University of Alberta, Edmonton, AB, Canada T6G 2E3

<sup>b</sup>Agricultural Research Service, USDA, Watkinsville, GA, 30677, USA

Received 7 December 2004; accepted 25 April 2005

### Abstract

We use an inverse-dispersion technique to diagnose gas emissions (ammonia) from a swine farm. A backward Lagrangian stochastic (bLS) model gives the emission-concentration relationship, so that downwind gas concentration establishes emissions. The bLS model takes as input the average wind velocity and direction, surface roughness, and atmospheric stability. Despite ignoring wind complexity and assuming a simplified source configuration in the model calculations, we argue that with concentration and wind measured sufficiently far from the farm the errors can be relatively small. An important part of our analysis was identifying periods likely to give erroneous results. The resulting emission calculations (6.5 and 16 g animal<sup>-1</sup> day<sup>-1</sup> in March and July, respectively) are plausible in the light of comparative figures.

© 2005 Elsevier Ltd. All rights reserved.

**Keywords:** Lagrangian stochastic models; Inverse-dispersion; Trace gas; Ammonia emissions; Monin–Obukhov similarity theory; Dispersion models

### 1. Introduction

Gas emissions from a farm to the atmosphere are difficult to measure directly. One complication is that farms are often a superposition of diverse emission sources, such as barns and waste storage facilities. One could concentrate on measuring these sources in isolation using, for instance, a mass balance or tracer technique for barns (e.g., Sharpe et al., 2001; Kaharabata and Schuepp, 2000), and micrometeorological or chamber techniques for outdoor sources (e.g., Aneja et al., 2001; Harper et al., 2000). But the effort in making such an inventory can be considerable. Another strategy would be to measure the totality of emissions by a mass

balance calculation, using wind and concentration measurements taken in a vertical plane downwind of the farm (Phillips et al., 2000). Yet to fully capture the emission plume from real-sized farms would require a measurement plane extending many meters above ground. Is there a simpler measurement technique?

Consider the hypothetical problem in Fig. 1, with an area source emitting gas at a continuous and unknown rate  $Q$  (kg s<sup>-1</sup>). Let us choose a point  $M$  within the emission plume where the time-average gas concentration above background ( $C - C_b$ ) is measured. With an atmospheric dispersion model prediction of the ratio of concentration at  $M$  to the source emission rate,  $(C/Q)_{\text{sim}}$ , one can infer the emission rate as:

$$Q = \frac{C - C_b}{(C/Q)_{\text{sim}}} \quad (1)$$

\*Corresponding author. Fax: +1 780 492 2030.

E-mail address: [thomas.flesch@ualberta.ca](mailto:thomas.flesch@ualberta.ca) (T.K. Flesch).

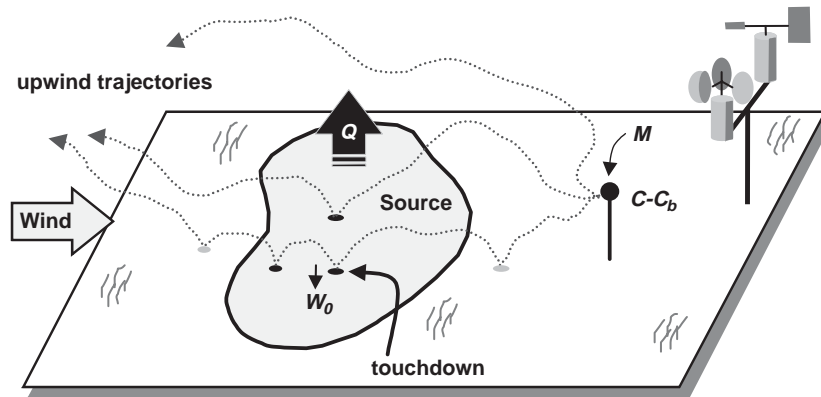


Fig. 1. The inverse-dispersion technique for estimating emission rate ( $Q$ ). Concentration rise above background ( $C - C_b$ ) is measured at  $M$ . The ratio  $(C/Q)_{\text{sim}}$  is calculated with a dispersion model. In a bLS model trajectories are calculated upwind of  $M$ , and  $(C/Q)_{\text{sim}}$  is given by trajectory “touchdowns” inside the source ( $w_0$  is the vertical velocity at touchdown).

This is the basis of the inverse–dispersion technique. It requires only a single measurement ( $C - C_b$ ) downwind of the source, with flexibility in the measurement location  $M$ .

In this paper we apply an idealized inverse–dispersion technique to calculate ammonia emissions from a swine nursery farm. We begin with a general discussion of the technique, the assumptions needed to make the technique practical in a farm setting, and limitations to its use.

## 2. Ideal vs. real terrain

Prediction of  $(C/Q)_{\text{sim}}$  in Eq. (1) is not trivial. Different types of dispersion models (e.g., Gaussian plume, K-theory) make this calculation with different levels of sophistication. In more realistic models one must furnish the average wind and turbulence statistics of the atmosphere—a difficult proposition. But for short-time intervals in a horizontally homogeneous surface layer (height  $z \lesssim 50$  m, but above a plant canopy), Monin–Obukhov similarity theory (MOST) states that the statistical properties of the wind are determined by a few key parameters (Garratt, 1992) which can be found by surface observations: the friction velocity  $u^*$ , the Obukhov stability length  $L$ , and the surface roughness length  $z_0$  (and we add the average wind direction  $\beta$  for a complete description). An example of an ideal surface layer application is given by Flesch et al. (2004), who calculated emissions from concentration measured downwind of an area source in simple terrain. A backward Lagrangian stochastic (bLS) model gave  $(C/Q)_{\text{sim}}$ . After eliminating periods when MOST relationships are inaccurate (i.e., extreme stabilities and low winds), the diagnosed emission rate  $Q_{\text{bLS}}$  overpredicted  $Q$  by an average of only 2%.

A real farm presents complications for a technique that assumes an idealized atmosphere. A variety of structures (buildings, trees, etc.) can create vortices, jets, and sheltered zones. How should this complexity be addressed? While it is possible to rigorously model dispersion in these environments, it requires specifying the spatially complex wind field. This is a difficult task. Comprehensive measurement of winds around a farm is beyond practical capabilities, and the alternative of modeling the wind is a complicated undertaking that gives predictions that may not be accurate (e.g., Wilson and Yee, 2003).

Another complication with real farms is the source configuration. As described here the inverse–dispersion technique calculates a single emission rate  $Q$ . With a compound source one must make assumptions about the component emission rates and their spatial configuration. For instance, one might assume that area sources have the same areal emission rate, or the farm can be treated as a set of identical point sources, etc. Such assumptions carry the risk of error in a  $Q$  inference.<sup>1</sup>

## 3. Neglecting complexity: move downwind

### 3.1. Wind complexity

Consider a farm within a nominally homogeneous landscape, i.e., farm structures locally disturb the wind but there is a downwind return to a spatially representative ambient state (i.e., where MOST is valid). We postulate that at some distance the set of tracer

<sup>1</sup>Inverse–dispersion methods can be generalized to deduce an apportionment of emissions within a complex, but this is a more difficult problem (e.g., Lehning et al., 1994).

trajectories emitted from the farm is not significantly different from that emitted from an equivalent undisturbed location. If measurement point  $M$  is beyond this threshold we can ignore the wind disturbance and take advantage of the simplicity of an idealized calculation of  $(C/Q)_{sim}$ . The most important factor in determining this distance is expected to be the height of the farm obstacles  $h$  (e.g. barn or trees), since the rate of wind “recovery” behind objects is known to scale on  $h$ .

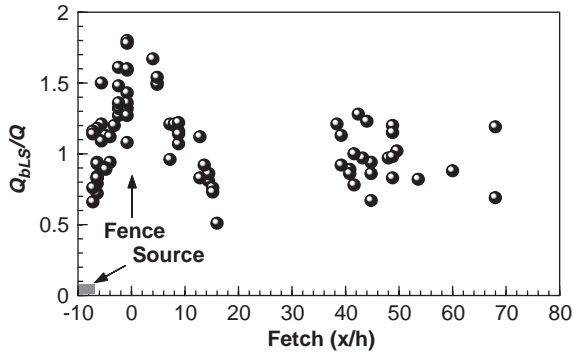


Fig. 2. Ratio of predicted to actual emission rate  $Q_{bLS}/Q$  plotted versus the downwind distance of the concentration measurement (fetch). The surface emission source (6 m × 6 m area source) was surrounded by a windbreak fence, and the fetch is scaled on the fence height  $h$ , and set to zero at the downwind fence location (when  $x/h < 0$ , concentration was measured in the fenced plot).

Flesch et al. (2005) conducted an experiment with a tracer source surrounded by an  $h = 1.25$  m tall windbreak fence that disturbed the wind. An idealized bLS dispersion model that did not account for the wind disturbance was used to diagnose the emission rate  $Q_{bLS}$ . Systematic errors of about 50% occurred when  $Q_{bLS}$  was calculated from concentration measured near the fence (Fig. 2). But when measured beyond  $5h$  from the fence, the average  $Q_{bLS}$  was only 2% different from the actual emission rate. Following from Flesch et al., we conclude that if concentration is measured beyond about  $10h$  from a farm, ignoring the local wind complexity will result in only a small error in the emissions inference.

### 3.2. Source complexity

Another advantage to moving away from a source complex is decreasing sensitivity to how one models the source configuration—details we do not generally know in advance. Intuition says that at some distance from a complex the component source plumes blend and become practically indistinguishable from a single source plume with the same aggregate emission rate. For example, Phillips et al. (2000) refers to van Ouwkerk (1993) when stating that for measurements beyond a distance of 10 farm heights or widths, a farm can be approximated as a single point source.

Consider the hypothetical farm in Fig. 3, consisting of two 4000 m<sup>2</sup> area sources emitting tracer at 1 and

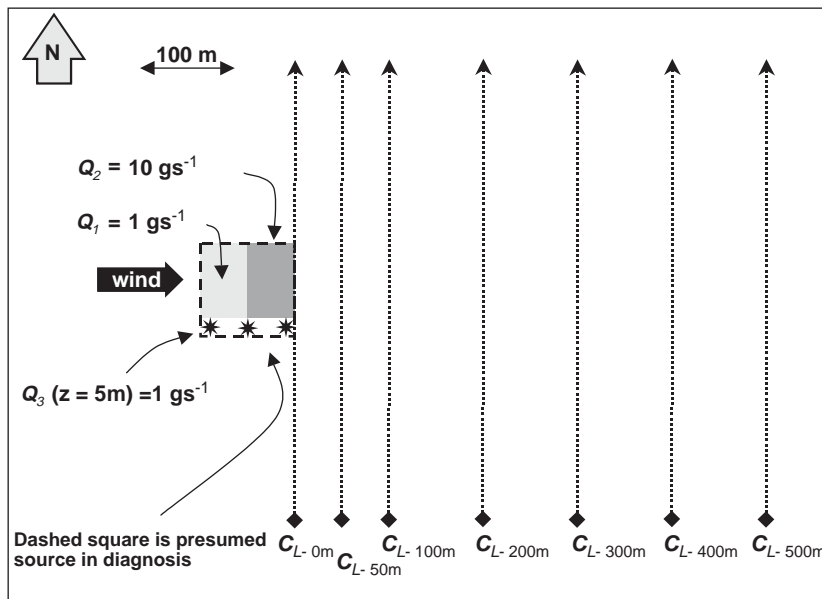


Fig. 3. Hypothetical emission complex: two surface area sources (emission rates  $Q_1$  and  $Q_2$ ) and three elevated point sources (each having emission rate  $Q_3$ ). Line-average concentration  $C_L$  is calculated at the illustrated positions using a dispersion model. These  $C_L$  are then used to deduce the total complex emission rate, assuming a single area source given by the dashed line.

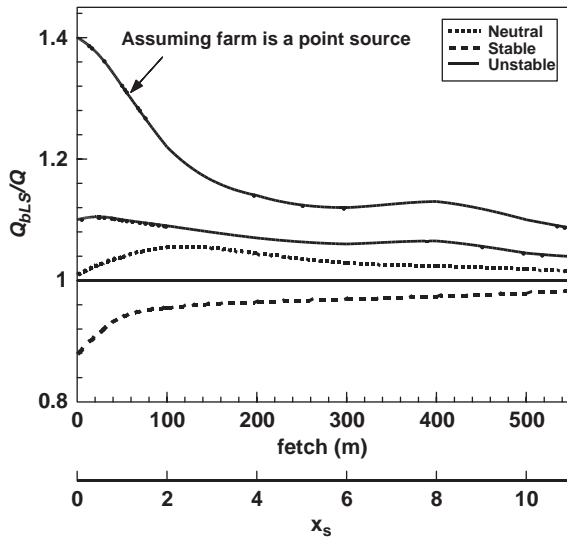


Fig. 4. Ratio of inferred to actual emission rate ( $Q_{\text{bLS}}/Q$ ) for hypothetical farm complex in Fig. 3, plotted versus distance from the farm boundary to  $C_L$  (fetch). Three atmospheric stratifications are considered: neutral ( $L = \infty$ ), stable ( $L = 10$  m), and unstable ( $L = -10$  m). Curves are hand-drawn fits. Top line gives  $Q_{\text{bLS}}$  if the complex is treated as a point source (in unstable conditions). Fetch is also displayed as a ratio of the source separation distance  $x_s$ .

$10 \text{ g s}^{-1}$ , and three elevated point sources ( $z = 5$  m) each emitting at  $1 \text{ g s}^{-1}$ . At what distance can we safely assume this farm complex is a single uniform area source that occupies the farm area? A bLS dispersion model (Section 4.3) is used to calculate line-average concentrations  $C_L$  (e.g., an open-path laser) downwind of the farm using the actual source configuration for moderately stable, unstable, and neutral atmospheric conditions. The same bLS model is then used to “back calculate” a total emission rate  $Q_{\text{bLS}}$ , but falsely assuming the farm is a single  $10,000 \text{ m}^2$  area source. Here we ignore the potential for wind complexity.

Fig. 4 shows how the accuracy of  $Q_{\text{bLS}}$  for this hypothetical farm depends on the location of  $C_L$ . As  $C_L$  is measured further downwind there is the expected trend toward greater accuracy (a fortuitous configuration make the neutral case an exception). But note that even with  $C_L$  taken adjacent to the farm ( $C_{L-0\text{m}}$ ), the error due to our incorrect source configuration is only about 10–150%. At 500 m from the farm the error drops to approximately 5%.

When considering the distance necessary to simplify the source configuration, an important scale will be the separation distance between the source components ( $x_s$ ). This will relate to the distance at which plume-blending occurs. In our example the east–west separation between the center of the two area sources ( $x_s = 50$  m) is the largest distance (north–south averaging in  $C_L$  makes the

north–south separation irrelevant). Extrapolating from Fig. 4 we speculate that with  $C_L$  measured beyond  $2x_s$  from the farm, the error from an incorrect source configuration is less than 10%. Generalizing from this example is questionable. If the disparity in component emission rates were smaller we could get closer and achieve the same accuracy, and vice versa. In contrast, if our modeled source configuration was less realistic, e.g., a point source instead of the area source, we would expect to have to go further downwind.<sup>2</sup>

#### 4. Implementation at actual farm

We conclude that with careful selection of a measurement location, an idealized inverse–dispersion technique can give the emissions from a farm complex within an error of  $\pm 10\%$  (on average). A first requirement is that the farm be isolated on the landscape, so that wind disturbances associated with the farm are local, with a downwind return to ambient winds. Meteorological observations ( $u^*$ ,  $z_0$ ,  $L$ , and  $\beta$ ) are to be made in the ambient regime. Isolation would also ensure that no nearby tracer sources confound the concentration observations. Another requirement is that concentration be measured many obstacle heights  $h$  downwind of the farm (we conservatively propose  $20h$ ). A third requirement is that concentration be measured multiple “source-separation” distances  $x_s$  downwind of the farm (a location beyond  $2x_s$  gave errors less than 10% in our earlier example).

##### 4.1. Swine nursery farm

Ammonia emissions are diagnosed from a swine nursery farm in the western United States. Located in a desert valley (elevation 1500 m), the farm consists of a single barn with two effluent lagoons (Fig. 5). Emissions are calculated for 5–6 July 2002 and 11–14 March 2003. There were 12,256 piglets on-site during July (averaging 14 kg per animal) and 11,664 in March (averaging 16 kg per animal). The site is ideal for our application. The terrain is flat and uniform around the farm, with a sparse coverage of low sagebrush. The area was mapped with a GPS unit. For prevailing southwest winds, only a smaller farm is 4 km upwind.

A low berm surrounds the lagoons, rising about 1 m above the surrounding landscape (and the lagoon surface). The barn is the dominant obstacle to wind flow, and we take its height  $h = 6$  m as our scaling height. The other important scale is the separation distance  $x_s$  between the barn and lagoons (in the alongwind direction). For southwest winds  $x_s$  between

<sup>2</sup>Treating our hypothetical farm as a point source would mean we must go  $\sim 10x_s$  downwind for  $Q_{\text{bLS}}$  to be within 10% of  $Q$  in the unstable case (Fig. 4).

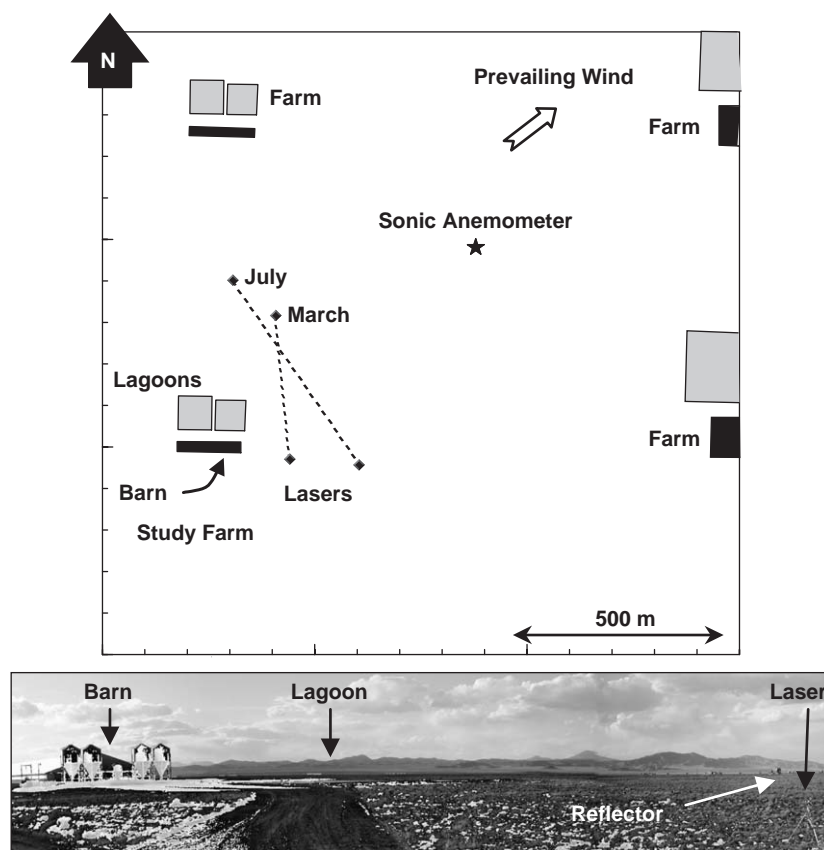


Fig. 5. Experimental layout at the nursery farm (barn and two lagoons). Laser paths were located northeast of the farm so emissions can be diagnosed for prevailing southwest winds. Meteorological information came from a sonic anemometer.

the center of the lagoons, and between the northeast lagoon and the barn center, is 50 and 90 m respectively.

#### 4.2. Concentration observations

Ammonia concentration was measured with an open-path laser (GasFinders, Boreal Laser Inc., Edmonton, Canada).<sup>3</sup> The line-average concentration between the laser and a distant retroreflector was processed to give 15-min averages ( $C_L$ ). To convert reported mixing-ratio concentrations ( $\text{ppm}_v$ ) to absolute concentration ( $\text{g m}^{-3}$ ) we use measured air temperature  $T$  and assume an atmospheric pressure of  $P = 840$  hPa:

$$C_L(\text{g m}^{-3}) = \frac{P m_w}{RT} \frac{1}{10^6} C_L(\text{ppm}), \quad (2)$$

where  $m_w$  is the molecular weight of  $\text{NH}_3$  ( $17.03 \text{ g mol}^{-1}$ ) and  $R$  is the molar gas constant ( $8.314 \text{ m}^3 \text{ Pa mol}^{-1} \text{ K}^{-1}$ ). Background concentration  $C_b$

was assumed to be insignificant (this was corroborated when the wind brought “fresh-air” over the laser path).

The laser and reflector were placed northeast of the farm in anticipation of the prevailing southwest winds (see Fig. 5). For a southwest wind the laser path was a minimum of 115/145 m downwind of the lagoon/barn in March, and 145/210 m in July. This puts  $C_L$  more than 20 h downwind of the barn, and a minimum of 1.2  $x_s$  from the farm boundary (if  $x_s$  is the lagoon–barn distance; or 2.2  $x_s$  if we use the lagoon–lagoon separation). The laser pathlength was 536 m (July) or 348 m (March). The laser and reflector was set at either  $z_m = 1.7$  or 1.8 m above ground.

#### 4.3. bLS dispersion model

A bLS dispersion model is used to calculate  $(C/Q)_{\text{sim}}$  for each 15-min  $C_L$  observation. We used the software “WindTrax” (Thunder Beach Scientific, Nova Scotia, Canada) which combines an interface where sources and sensors are mapped, with the bLS model described by Flesch et al. (2004). In the bLS model thousands of

<sup>3</sup>Listing of source names does not imply endorsement or preferential treatment by the University of Alberta or the United States Department of Agriculture.

trajectories are calculated upwind of the laser path for the prevailing wind conditions ( $u^*$ ,  $L$ ,  $z_0$ ,  $\beta$ ). For an area source the important information is where the trajectories intersect the ground (“touchdowns”) and their associated vertical velocity ( $w_0$ ):

$$(C_L/Q)_{\text{sim}} = \frac{1}{N} \sum \left| \frac{2}{w_0} \right|, \quad (3)$$

where  $N$  is the number of computed trajectories (released evenly along the laser path), and the summation covers only touchdowns within the source (Fig. 1).<sup>4</sup> The touchdowns map the concentration “footprint”, i.e., the ground area where emissions influence concentration. We do not mimic ammonia deposition to ground, which should be small given the dry conditions, sparse vegetation, and short distances involved.

In our bLS simulations the farm is represented as three surface area sources: the two lagoons and the area occupied by the barn. Each is assumed to have the same areal emission rate, so that touchdowns in any of these areas are counted equally in Eq. (3). This treatment is undoubtedly in error. The two lagoons (primary and secondary waste treatment) will have different emission rates, and the barn is not an area source (emissions occur from vents on the north and south walls). However, following the arguments in Section 3.2, we assume that with our  $C_L$  location sufficiently far from the farm we are insensitive to these simplifications (we will return to this question in Section 6).

#### 4.4. Meteorological observations

The WindTrax bLS model requires as input the average alongwind velocity  $U$  (at an arbitrary height),  $L$ ,  $z_0$ , and  $\beta$ . A 3-D sonic anemometer (CSAT-3, Campbell Sci.) provided this information. The anemometer was placed at height  $z_{\text{son}} \sim 2$  m (height varied slightly from 2002 to 2003), and wind velocity and temperature were sampled at a frequency of 16 Hz. Velocity and heat flux statistics were transformed into along/across wind coordinates using two coordinate rotations (yaw and pitch corrections, e.g., Kaimal and Finnigan, 1994), and we calculate:

$$\begin{aligned} u_* &= \sqrt[4]{\langle u'w' \rangle^2 \langle v'w' \rangle^2}, \\ L &= -\frac{u_*^2 T}{k_v g \langle w'T' \rangle}, \\ z_0 &= \frac{z_{\text{son}}}{\exp(Uk_v/u_* - \psi)}, \end{aligned} \quad (4)$$

where  $\langle u'w' \rangle$  and  $\langle v'w' \rangle$  are velocity fluctuation covariances (see Garratt, 1992),  $T$  is the average acoustic air temperature given by the sonic anemometer,  $k_v$  is von Karman’s constant (assumed to be 0.4),  $g$  the gravitational

constant,  $\langle w'T' \rangle$  the vertical sensible heat flux, and  $\psi$  a stability correction for the log wind profile (given in Flesch et al., 2004). The sonic observations also provided velocity standard deviations ( $\sigma_{u,v,w}$ ) which we later use in the bLS model.

## 5. Data filtering

Not all observation periods provide good emission estimates. Here we discuss the data filtering process for our March observations, which span 295 consecutive 15-min periods (Fig. 6a). Twelve of these periods had no  $C_L$  measurement due to the laser and reflector being misaligned (e.g., heating/cooling of tripods). During another 94 periods the farm plume was blown away from the laser path, with no possibility of an emission inference. This leaves a base of 189 observations. The average emission rate calculated with these periods is  $Q_{\text{bLS}} = 10.6 \text{ g s}^{-1}$ , with a standard deviation in the 15-min estimates of  $118.4 \text{ g s}^{-1}$ . This emission rate, which dramatically overestimates the actual emissions, will drop considerably as we employ a series of quality filters.

### 5.1. Removing periods of MOST inaccuracy

Accurate  $Q_{\text{bLS}}$  depends on the accuracy of the MOST-based relationships that underlie the bLS model. These are known to be unreliable during extreme stability. For instance, Flesch et al. (2004) found  $Q_{\text{bLS}}$  predictions were inaccurate when  $|L| \leq 2$  m. They also found that  $u_* \leq 0.15 \text{ m s}^{-1}$  was associated with inaccuracy. We therefore remove from our analysis 58 periods with  $|L| \leq 2$  m or  $u_* \leq 0.15 \text{ m s}^{-1}$ . This eliminates many previous  $Q_{\text{bLS}}$  outliers (Fig. 6b) and dramatically drops the average  $Q_{\text{bLS}}$  from 10.6 to  $1.69 \text{ g s}^{-1}$ , and gives a standard deviation of  $1.23 \text{ g s}^{-1}$ .

### 5.2. Removing periods of unrepresentative sampling

In some periods the farm plume only “glances” the laser path. This causes two problems. First is that the plume edge carries greater  $(C/Q)_{\text{sim}}$  uncertainty, since extreme trajectories at the plume margin are by definition less predictable. In addition the edge of the plume is associated with emissions from only the farm edge, giving a poor estimate of the whole-farm average. To identify such periods we visually assess the bLS touchdown catalog for each period (see Fig. 7), and accept only cases with touchdown coverage in some of each source area (i.e., barn or lagoons). There are 23 periods identified as having poor touchdown coverage. Eliminating these removes several  $Q_{\text{bLS}}$  outliers (Fig. 6c), and the average  $Q_{\text{bLS}}$  drops slightly from 1.69 to  $1.59 \text{ g s}^{-1}$  (but with a more significant reduction in the standard deviation from 1.23 to  $0.81 \text{ g s}^{-1}$ ).

<sup>4</sup>Here the units of  $Q$  are  $\text{g m}^{-2} \text{ s}^{-1}$ , but henceforth we multiply the areal emission rate by the source area and report an area-integrated  $Q$  with units of  $\text{g s}^{-1}$ .

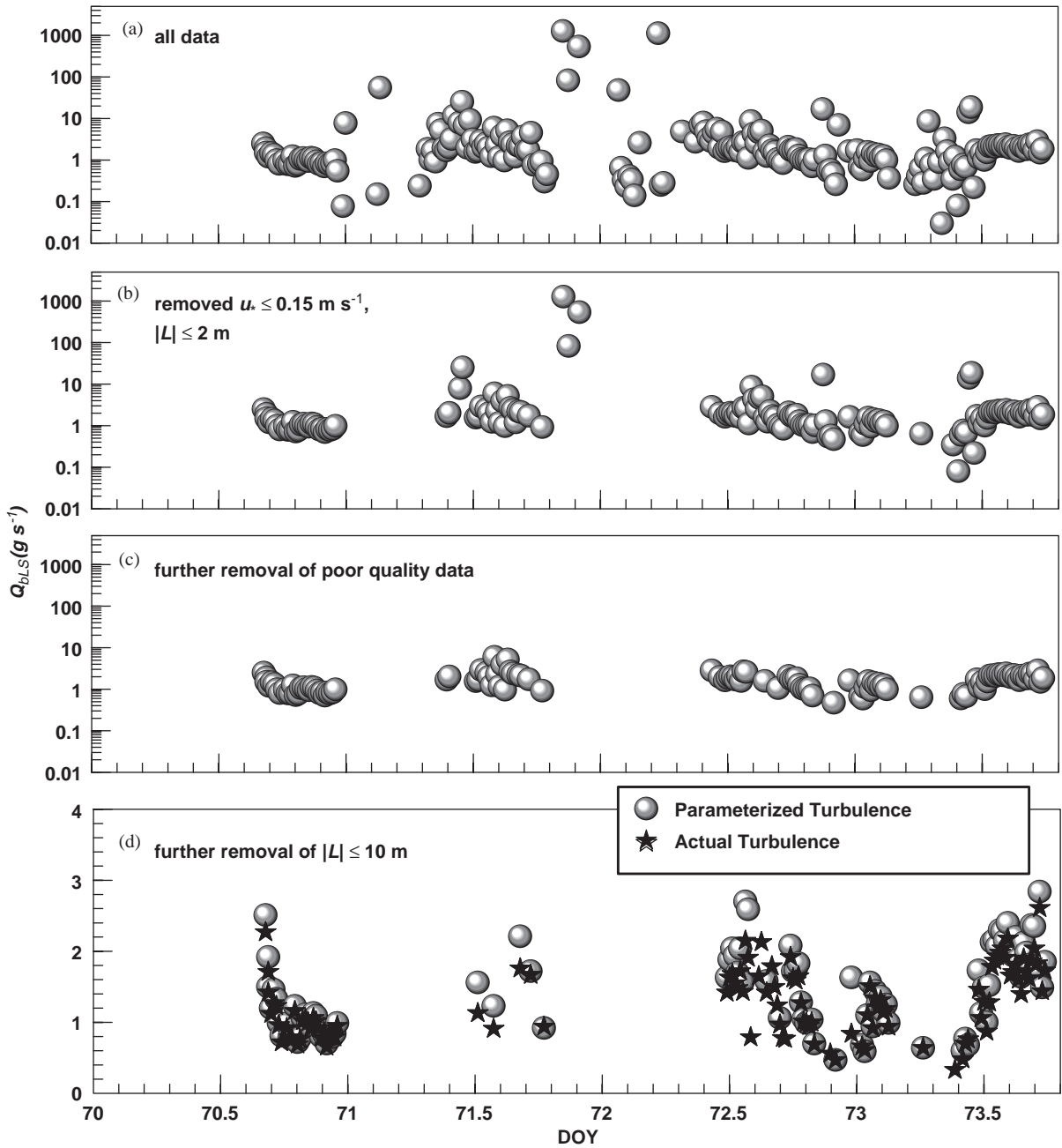


Fig. 6. Farm ammonia emission rate ( $Q_{bLS}$ ) versus day-of-the-year (DOY) during March: (a) complete data set; (b) removed periods with  $u^* \leq 0.15 \text{ m s}^{-1}$  or  $|L| \leq 2 \text{ m}$ ; (c) further removal of periods with poor touchdown coverage (log scale); (d) further removal of periods with  $|L| \leq 10 \text{ m}$ . In (d) we also display  $Q_{bLS}$  calculated using actual turbulence (switched to a linear scale for  $Q_{bLS}$ ).

### 5.3. Further removal of unstable periods

Now consider the relationship between our filtered  $Q_{bLS}$  and wind velocity  $U$  (Fig. 8). With lagoon emissions we expect a strong positive correlation

between the two (e.g., Denmead et al., 1982; Harper et al., 2000), and a naturally ventilated barn (describes our barn much of the time) should exhibit a similar dependence. On average we see the expected correlation, but we also see exceptions having a large  $Q_{bLS}$  but

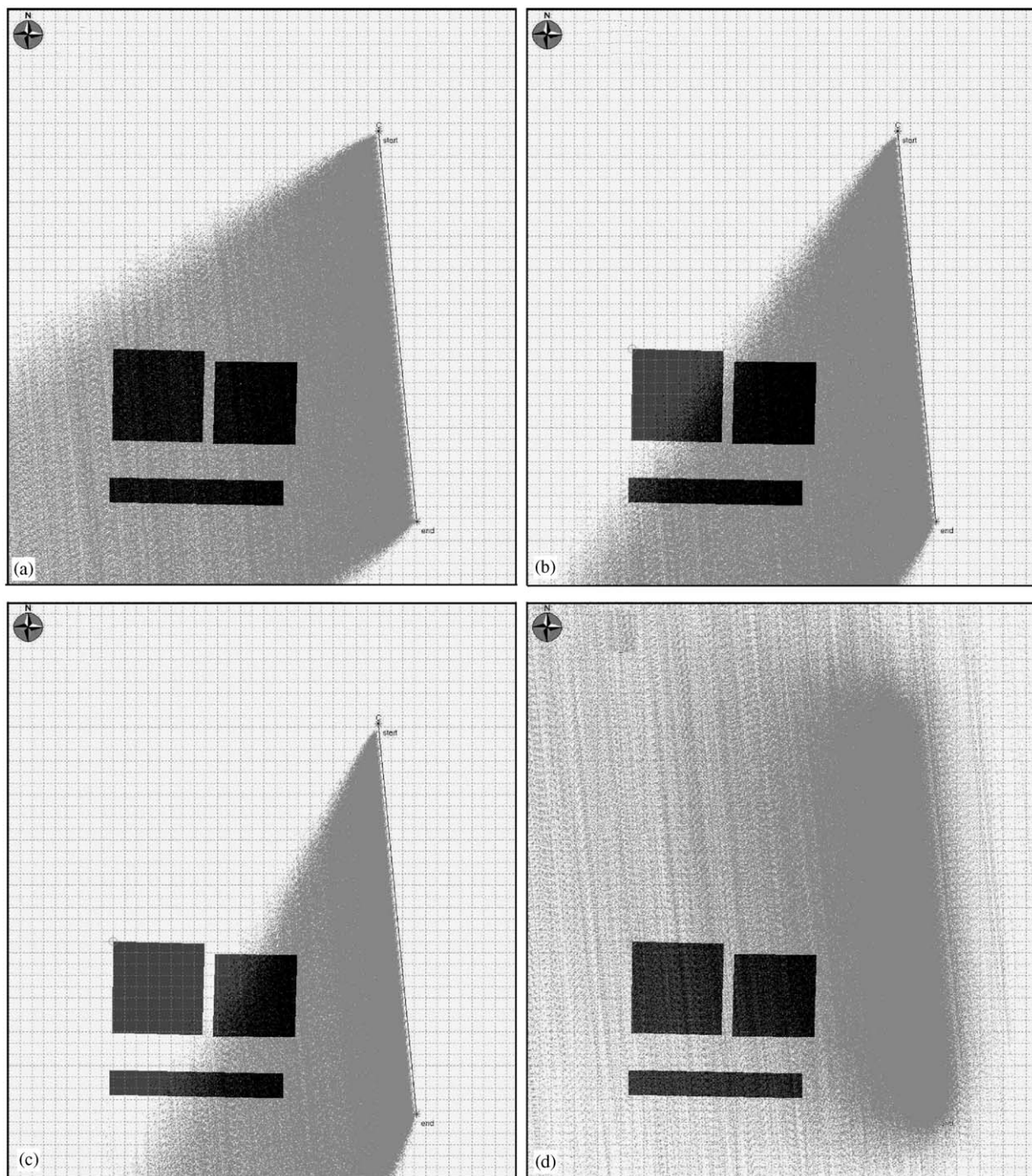


Fig. 7. Example touchdown catalogs: (a) and (b) are “good” quality data with touchdowns in all three source areas; (c) a “poor” quality example with no touchdowns in the northwest lagoon; and (d) in very unstable conditions the touchdowns are weighted toward the northeasterly lagoon.

low  $U$ . These outliers correspond to strongly unstable conditions ( $-10 < L < 0$  m). We consider three possibilities:

1. The  $Q_{\text{BLS}}$  outliers are accurate. High emissions (but low winds) could result from exhaust fans operating in the barn, overturning of the lagoon effluent, etc.

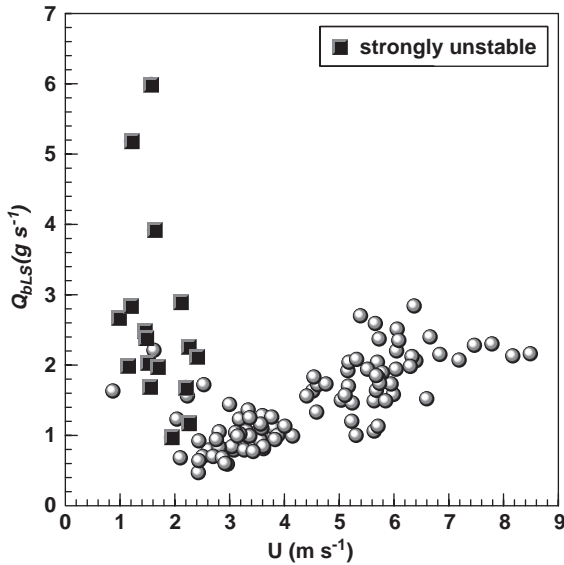


Fig. 8. Predicted ammonia emission rate  $Q_{bLS}$  (March) versus the average horizontal wind velocity  $U$  (measured at  $z = 2$  m). Periods of strongly unstable atmospheric conditions ( $-10 \text{ m} < L < 0 \text{ m}$ ) are given separate symbols.

Outliers are concentrated on Day 71, when there is evidence that barn fans were running.

2. These estimates are unrepresentative. In strongly unstable conditions the  $C_L$  footprint is compressed nearer the laser path, with touchdowns concentrated in the northeasterly lagoon (Fig. 7d). Then  $Q_{bLS}$  is overweighted toward this lagoon’s emissions (the primary lagoon) and not representative of the whole-farm.
3. The bLS model is inaccurate. A common presumption is that MOST descriptions are inaccurate for  $z > |L|$ . Following Flesch et al. (2004) we eliminated periods with  $|L| \leq 2 \text{ m}$  (very stable or unstable). But if a large proportion of trajectories traveling from the farm to the laser path rise above  $z = 2 \text{ m}$ , this limit may be insufficient. Because our problem dimensions are larger than Flesch et al., we may need a larger  $|L|$  threshold.

On the presumption that explanations 2 or 3 are more likely, we expand our stability rejection criterion from  $|L| \leq 2 \text{ m}$  to  $|L| \leq 10 \text{ m}$ . The effect of this more stringent criterion is to reduce by 16 the number of observations periods (Fig. 6d). The average  $Q_{bLS}$  then drops from  $1.59$  to  $1.44 \text{ g s}^{-1}$  (with the standard deviation reduced from  $0.81$  to  $0.57 \text{ g s}^{-1}$ ).

#### 5.4. Using actual turbulence observations

The bLS model uses the input  $U$ ,  $L$ , and  $z_0$  (selected to insure the correct  $u^*$ ) to calculate the needed wind

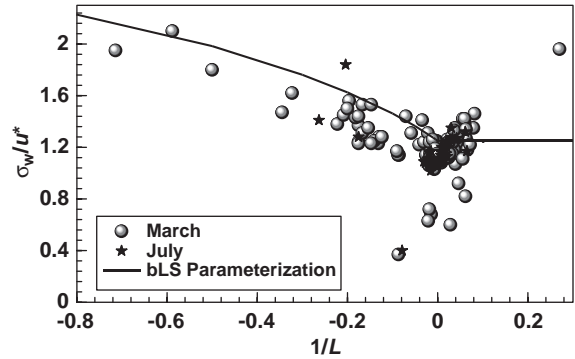


Fig. 9. Standard deviation of vertical velocity  $\sigma_w$  (normalized on friction velocity  $u^*$ ) plotted against stability (the reciprocal of the Obukhov length  $L$ ). Symbols represent March and July observations, and the line gives the default bLS parameterization with  $b_w = 1.25$ .

statistics, including the standard deviations of velocity fluctuations ( $\sigma_{u,v,w}$ ). Scaling constants  $b_{u,v,w}$  are used in the model, with  $\sigma_{u,v,w}/u^* = b_{u,v,w}$  in neutral conditions. We initially used traditional  $b_{u,v,w}$  ( $= 2.5, 2.0, 1.25$ ), which is the WindTrax default. However, we found this overestimated  $\sigma_w$  by an average of 10% (Fig. 9). We therefore re-compute  $Q_{bLS}$  using  $b_{u,v,w}$  adjusted on a period-by-period basis to reproduce the observed turbulence (described in Flesch et al., 2004).

The “tuning” of the bLS model has two effects. Altering  $\sigma_v$  (crosswind fluctuations) alters the spread of the touchdown catalog, and some of the previous “good” data becomes “poor” and vice versa (in terms of a representative sampling of the farm). Overall we find a gain of “good” data from 92 to 102 periods. The other effect is a change in  $Q_{bLS}$  (Fig. 6d), with the average  $Q_{bLS}$  reduced from  $1.44$  to  $1.27 \text{ g s}^{-1}$  (with standard deviation reduced from  $0.57$  to  $0.49 \text{ g s}^{-1}$ ).

## 6. Source configuration revisited

In our calculations we have assumed a source configuration for the farm. Our earlier example (Section 3.2) demonstrated how the sensitivity of  $Q_{bLS}$  to configuration details is reduced as concentration is measured further from the farm. Up to this point we have assumed our  $C_L$  observations are far enough to justify treating the farm as three area sources with identical areal emission rates. We now re-examine this assumption with our actual farm configuration. First we consider a modification of our analysis, to avoid assuming the barn and lagoons have equal emission rates.

An inverse-dispersion technique can theoretically diagnose multiple emission rates if given multiple concentration observations (e.g. Lehning et al., 1994).

With three observations we could infer separate emission rates  $Q_B$  (barn),  $Q_{L-nw}$ , and  $Q_{L-ne}$  (northwest and northeast lagoons). We try this by taking three consecutive 15-min  $C_L$  observations and assuming emissions were constant over the 45 min, writing:

$$\begin{aligned} \left(\frac{C_L}{Q_B}\right)_1 Q_B + \left(\frac{C_L}{Q_{L-ne}}\right)_1 Q_{L-ne} + \left(\frac{C_L}{Q_{L-nw}}\right)_1 Q_{L-nw} &= (C_L)_1, \\ \left(\frac{C_L}{Q_B}\right)_2 Q_B + \left(\frac{C_L}{Q_{L-ne}}\right)_2 Q_{L-ne} + \left(\frac{C_L}{Q_{L-nw}}\right)_2 Q_{L-nw} &= (C_L)_2, \\ \left(\frac{C_L}{Q_B}\right)_3 Q_B + \left(\frac{C_L}{Q_{L-ne}}\right)_3 Q_{L-ne} + \left(\frac{C_L}{Q_{L-nw}}\right)_3 Q_{L-nw} &= (C_L)_3, \end{aligned} \quad (5)$$

where  $(C_L/Q_B)$  would be the ratio of concentration to emission rate for just the barn contribution,  $(C_L/Q_{L-ne})$  the relationship for just the northeast lagoon, etc. The subscripts 1–3 represent consecutive observation periods (i.e., the  $C_L/Q$  ratios vary as the wind changes). Each coefficient is determined by WindTrax.

When we thus analyze the  $C_L$  record we find Eqs. (5) do not yield realistic results. In every case at least one emission source is negative (e.g., in one 45-min period  $Q_B, Q_{L-ne}, Q_{L-nw} = -10.5, 3.7, 7.4 \text{ g s}^{-1}$ ) and there is tremendous temporal variability (e.g., in consecutive periods  $Q_B = -14.7, 9.6, -10.5 \text{ g s}^{-1}$ ). These inaccuracies are the result of an ill-conditioned system: the inferred  $Q$  are extremely sensitive to uncertainties in the  $C_L/Q$  coefficients. This can be quantified by the condition number ( $N_c$ ), which is interpreted as the ratio of the uncertainty in calculated  $Q$  to the uncertainty in  $C_L/Q$  (Gerald and Wheatley, 1984). In this problem  $N_c$  ranges from 100 to 10,000. So if the bLS model calculates  $C_L/Q$  with 10% uncertainty (a reasonable generalization), the uncertainty in  $Q$ 's range from 1000% to 100,000%. This sensitivity is due to the geometry of our source/sensor layout, and the inability of this layout to differentiate the source components.<sup>5</sup>

We now consider three scenarios to delineate the potential error from our original assumption of identical areal emission rates from the barn and lagoons. The  $Q_{bLS}$  is recalculated for 8 h in March 2003 (afternoon-evening of day 70), but assuming emissions come exclusively from the barn or a lagoon. These results are then compared with  $Q_{bLS}$  assuming equal emission rates from all three sources. If emissions are only from the NW lagoon (secondary lagoon), but we falsely assume three equal emission rates, then the total farm emissions are underestimated by 43%. With emissions from only the NE lagoon (primary lagoon) we will overestimate emissions by 35%. And if the barn is the

only source, emissions are overestimated by only 2%. These worse-case scenarios show a potential error of order 40%, which indicates our measurement location should ideally have been further from the farm.

In our opinion ammonia emissions could not realistically be confined to one source area. Harper et al. (2004) for example, found equal emissions from the barn and lagoon of a swine farm in North Carolina. We suspect emissions are concentrated in the barn and the primary lagoon (NE lagoon). Taking more realistic relative emissions of total  $(Q_B, Q_{L-ne}, Q_{L-nw}) = (2, 2, 1)$  means our assumption of a homogeneous source would cause an overestimation in emissions by 9%. And the more emissions are weighted toward the barn, the more accurate  $Q_{bLS}$  becomes.

## 7. Farm emissions

We calculate ammonia emissions from the farm in March and July using the data filtering process described earlier: we eliminate periods with  $u^* \leq 0.15 \text{ m s}^{-1}$ ,  $|L| \leq 10 \text{ m}$ , or when  $C_L$  is unrepresentative of the whole-farm plume. We also use the observed  $\sigma_{u,v,w}$  for each period to modify the bLS model to reproduce the measured turbulence.

In March we have 102 observations of  $Q_{bLS}$  taken over four days (Fig. 10), with emissions ranging from 0.5 to  $2.8 \text{ g s}^{-1}$ . There is the strong correlation between emissions and wind speed discussed earlier, and we see a consistent mid-afternoon emission peak of  $2\text{--}3 \text{ g s}^{-1}$ . Emissions never drop below  $0.5 \text{ g s}^{-1}$ , perhaps because we eliminate low wind periods in our filtering, or maybe this represents a base emission rate from the animals. For all 102 observations the average  $Q_{bLS}$  is  $1.27 \text{ g s}^{-1}$ . Because our filtering preferentially removes nighttime periods, this average is weighted toward daytime conditions. To remedy this we approximate missing observations using the linear  $Q_{bLS}$  versus  $U$  relationship shown in Fig. 10c, and use  $U$  to estimate  $Q$ . For a 72 h subset we find an average  $Q_{bLS} = 0.9 \text{ g s}^{-1}$ , or  $6.5 \text{ g animal}^{-1} \text{ day}^{-1}$ .

Our July dataset spans only 15.5 h (early evening through late morning), with emissions ranging from 0.6 to  $6.3 \text{ g s}^{-1}$  (Fig. 10b). Again we see a strong correlation between  $Q_{bLS}$  and  $U$ . Interpolating and extrapolating from these observations using the polynomial  $Q_{bLS}$  versus  $U$  relationship in Fig. 10c, we calculate a 24-h average  $Q_{bLS} = 2.2 \text{ g s}^{-1}$ , or  $16 \text{ g animal}^{-1} \text{ day}^{-1}$ . This is a little over twice the March value (but from an admittedly small number of observations). While we see higher overall emissions in July than March, in both cases the lowest emission rate is about  $0.5 \text{ g s}^{-1}$ , an indication of a base emission rate.

How do these emissions compare with other studies? Our March and July averages of 6.5 and  $16 \text{ g animal}^{-1}$

<sup>5</sup>We tried adding more  $C_L$  observations by lengthening our analysis interval (up to 5 h), then calculating statistical best-fit solutions, but this did not improve our results. Perhaps if wind direction had changed more dramatically between periods we may have had more success in differentiating emissions.

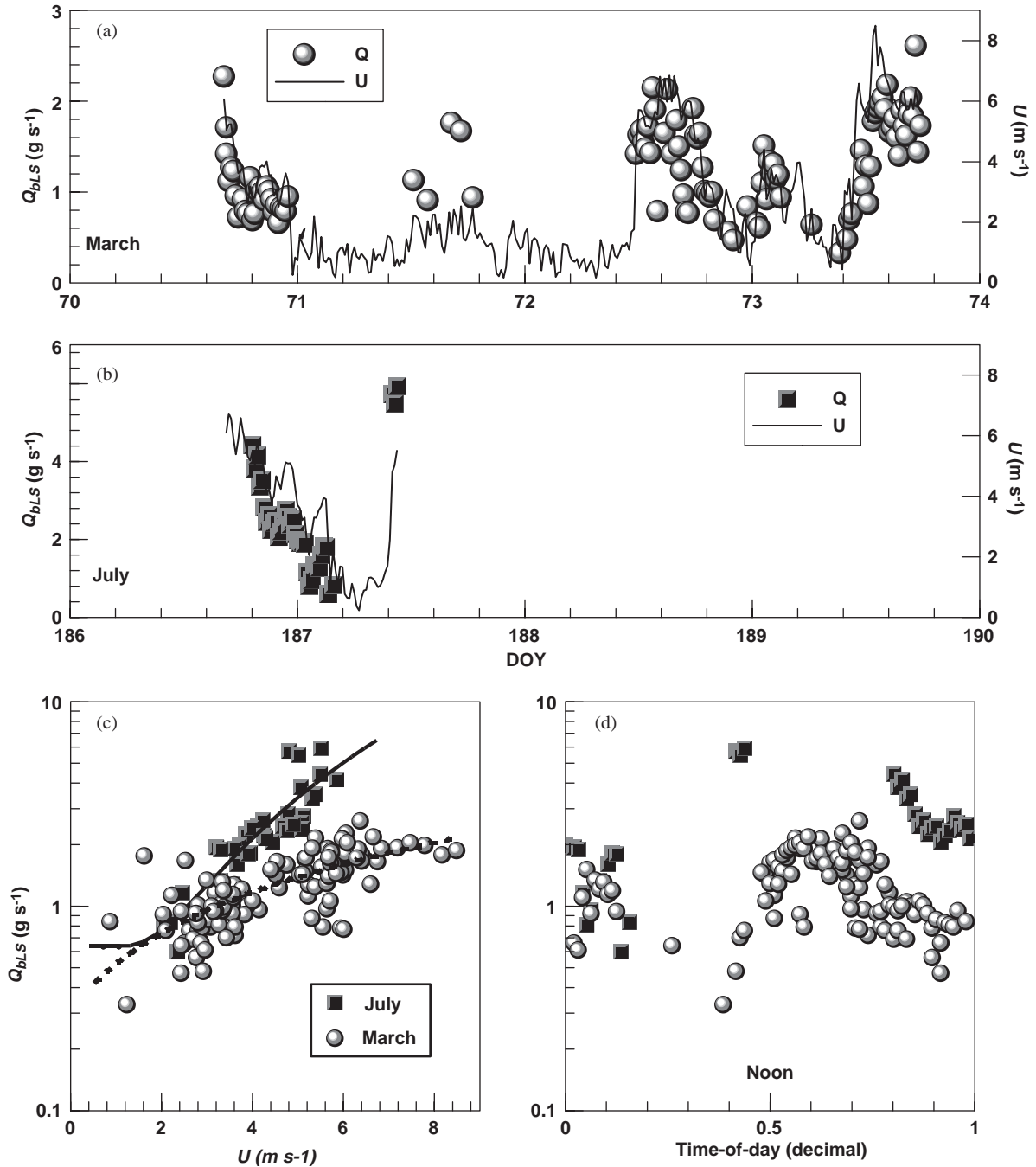


Fig. 10. Farm ammonia emission rate ( $Q_{bLS}$ ) plotted versus DOY during (a) March and (b) July (wind velocity  $U$  at  $z = 2$  m displayed as a line). The  $Q_{bLS}$  predictions are shown versus (c) wind velocity  $U$  and (d) local time-of-day (e.g. 0.5 is noon). The lines displayed in (c) are best-fit quadratic (July) and linear (March) regressions.

day<sup>-1</sup>, respectively, compare with generic emission factors for swine of 25.2 g animal<sup>-1</sup> day<sup>-1</sup> estimated by Battye et al. (1994) for the USA, 19.2 g animal<sup>-1</sup> day<sup>-1</sup> estimated by Doorn et al. (2002) for the USA, and 14.7 g animal<sup>-1</sup> day<sup>-1</sup> estimated for Europe by Asman

(1992). Our lower values are consistent with smaller nursery animals. The emissions are also broadly consistent with the observations of Harper et al. (2000) who found annual rates of 6.3 g animal<sup>-1</sup> day<sup>-1</sup> from the lagoon of a farrow-to-finish farm in Georgia (no

barn emissions). We interpret this consistency as a broad indication of the success of the bLS technique.

## 8. Summary and conclusions

We demonstrated the application of an inverse–dispersion technique to estimate ammonia emissions from a swine nursery farm. We argued that use of an idealized dispersion model, and an idealized treatment of the farm source configuration, is justified for this site. An important part of our analysis was identifying periods when  $Q_{\text{bLS}}$  was likely in error, because of either the potential for bLS model errors or unrepresentative concentration observations. After removing these questionable periods we calculated ammonia emissions of 6.5 and 16 g animal<sup>-1</sup> day<sup>-1</sup> in March and July, respectively. These values are consistent with other studies.

We found the bLS technique was easy to apply. The open-path laser was simple to use, and all necessary meteorological data were supplied by a 3-D sonic anemometer, easily placed on the surrounding landscape. Because the terrain was uniform, positioning the laser and anemometer was straightforward. Having a predominant wind direction also helped identify good measurement locations. In our experiment the data-quality filters resulted in the removal of more than half our observations, which highlights the importance of “gap-filling” procedures to approximate missing emissions when applying the technique in long-term studies.

The suitability of the technique in other situations will depend on the specific farm setting. Complex terrain would make the simple bLS model less defensible, and proper measurement locations less clear. And if the farm is surrounded by other emission sources it may become impossible to separate the farm tracer plume from a complex background pattern. But if one avoids such complex settings, then the inverse–dispersion technique can be an easy-to-use method for estimating whole-farm emissions.

## Acknowledgements

This work has been supported by research grants from the Natural Sciences and Engineering Research Council of Canada (NSERC) and the Canadian Foundation for Climate and Atmospheric Sciences (CFCAS).

## References

Aneja, V.P., Bunton, J., Walker, J.T., Malik, B.P., 2001. Measurement and analysis of atmospheric ammonia emissions from anaerobic lagoons. *Atmospheric Environment* 35, 1949–1958.

Asman, W.A.H., 1992. Ammonia emissions in Europe: updated emission and emission variations. National Institute of Public Health and Environmental Protection, Bilthoven, the Netherlands.

Battye, R., Battye, W., Overcash, C., Fudge, S., 1994. Development and selection of ammonia emission factors. EPA Contract No. 68-D3-0034. USEPA, Research Triangle Park, NC.

Denmead, O.T., Freney, J.R., Simpson, J.R., 1982. Dynamics of ammonia volatilization during furrow irrigation of maize. *Soil Science Society of America Journal* 46, 149–155.

Doorn, M.R.J., Natschke, D.F., Thorneloe, S.A., Southerland, J., 2002. Development of an emission factor for ammonia emissions from US swine farms based on field tests and application of a mass balance method. *Atmospheric Environment* 36, 5619–5625.

Flesch, T.K., Wilson, J.D., Harper, L.A., Crenna, B.P., Sharpe, R.R., 2004. Deducing ground-air emissions from observed trace gas concentrations: a field trial. *Journal of Applied Meteorology* 43, 487–502.

Flesch, T.K., Wilson, J.D., Harper, L.A., 2005. Deducing ground-air emissions from observed trace gas concentrations: a field trial with wind disturbance. *Journal of Applied Meteorology* 44, 475–484.

Garratt, J.R., 1992. *The Atmospheric Boundary Layer*. Cambridge University Press, New York 316pp.

Gerald, C.F., Wheatley, P.O., 1984. *Applied Numerical Analysis*. Addison-Wesley Publishing, Reading, MA 579pp.

Harper, L.A., Sharpe, R.R., Parkin, T.B., 2000. Gaseous emissions from anaerobic swine lagoons: ammonia, nitrous oxide, and dinitrogen gas. *Journal of Environmental Quality* 29, 1356–1365.

Harper, L.A., Sharpe, R.R., Parkin, T.B., Visscher, A.D., Van Cleemput, O., Byers, F.M., 2004. Nitrogen cycling through swine production systems: ammonia, dinitrogen, and nitrous oxide emissions. *Journal of Environmental Quality* 33, 1189–1201.

Kaharabata, S.K., Schuepp, P.H., 2000. Estimating methane emissions from dairy cattle housed in a barn and feedlot using atmospheric tracer. *Environmental Science and Technology* 34, 3296–3302.

Kaimal, J.C., Finnigan, J.J., 1994. *Atmospheric Boundary Layer Flows*. Oxford University Press, Oxford 289pp.

Lehning, M., Shonnard, D.R., Chang, D.P.Y., Bell, R.L., 1994. An inversion algorithm for determining area-source emissions from downwind concentration measurements. *Journal of the Air and Waste Management Association* 44, 1204–1213.

Phillips, V.R., Scholtens, R., Lee, D.S., Garland, J.A., Sneath, R.W., 2000. A review of methods for measuring emission rates of ammonia from livestock buildings and slurry or manure stores, Part 1: Assessment of basic approaches. *Journal of Agricultural Engineering Research* 77, 355–364.

Sharpe, R.R., Harper, L.A., Simmons, J.D., 2001. Methane emissions from swine houses in North Carolina. *Chemosphere—Global Change Science* 3, 1–6.

Van Ouwkerk, E.N.J., 1993. Meetmethoden ammonia emissie uit stallen. In: *Methods for measuring ammonia emissions from animal housing*. DLO, Wageningen, Netherlands.

Wilson, J.D., Yee, E., 2003. Calculation of winds disturbed by an array of fences. *Agricultural and Forest Meteorology* 115, 31–50.